Behavioral/Systems/Cognitive

Degeneracy and Neuromodulation among Thermosensory Neurons Contribute to Robust Thermosensory Behaviors in *Caenorhabditis elegans*

Matthew Beverly, Sriram Anbil, and Piali Sengupta
Department of Biology and National Center for Behavioral Genomics, Brandeis University, Waltham, Massachusetts 02454

Animals must ensure that they can execute behaviors important for physiological homeostasis under constantly changing environmental conditions. The neural mechanisms that regulate this behavioral robustness are not well understood. The nematode *Caenorhabditis elegans* thermoregulates primarily via modulation of navigation behavior. Upon encountering temperatures higher than its cultivation temperature (T_c), *C. elegans* exhibits negative thermotaxis toward colder temperatures using a biased random walk strategy. We find that *C. elegans* exhibits robust negative thermotaxis bias under conditions of varying T_c and temperature ranges. By cell ablation and cell-specific rescue experiments, we show that the ASI chemosensory neurons are newly identified components of the thermosensory circuit, and that different combinations of ASI and the previously identified AFD and AWC thermosensory neurons are necessary and sufficient under different conditions to execute a negative thermotaxis strategy. ASI responds to temperature stimuli within a defined operating range defined by T_c, and signaling from AFD regulates the bounds of this operating range, suggesting that neuromodulation among thermosensory neurons maintains coherence of behavioral output. Our observations demonstrate that a negative thermotaxis navigational strategy can be generated via different combinations of thermosensory neurons acting degenerately, and emphasize the importance of defining context when analyzing neuronal contributions to a behavior.

Introduction

Animals must maintain cellular and physiological homeostasis over a wide range of conditions. Although robustness can be achieved via dedicated networks that function only under specific conditions, this strategy does not generate reliable outputs when faced with unforeseen circumstances (Tononi et al., 1999). In contrast, degenerate systems, in which multiple distinct components contribute to the generation of the same output in a context-dependent manner, can permit adaptive flexibility and tolerate perturbation (Tononi et al., 1999; Edelman and Gally, 2001; Wagner, 2005; Whitacre, 2010). The role of degeneracy in generating robustness has been studied experimentally and theoretically (Hartman et al., 2001; Prinz et al., 2004; Wagner, 2005; Wagner and Wright, 2007), but much remains to be understood about the mechanisms that ensure behavioral robustness under varying conditions.

The nematode *Caenorhabditis elegans* exhibits a particularly robust and adaptable behavior on thermal gradients. *C. elegans* forms a memory of its cultivation temperature (T_c) and exhibits stereotyped behaviors at specific temperature ranges relative to T_c. At temperatures higher than T_c, worms move down the gradient toward colder temperatures in a behavior called negative thermotaxis (Hedgecock and Russell, 1975; Mori and Ohshima, 1995). T_c memory is plastic and can be reset upon cultivation at a different temperature (Hedgecock and Russell, 1975).

Modulation of locomotory behavior is the primary mode of thermoregulation in *C. elegans* (Ramot et al., 2008b). Given the critical role of temperature in regulating nearly all aspects of *C. elegans* physiology [e.g., Klass (1977), Golden and Riddle (1984), and van der Linden et al. (2010)], it is essential that worms maintain their body temperature within a physiologically optimal range. Theoretical simulations have shown that negative thermotaxis is remarkably robust and resistant to environmental perturbations or to genetic changes affecting the animals' locomotion (Ramot et al., 2008b). Indeed, systematic analyses of negative thermotaxis indicate that worms can exhibit this behavior over varying conditions such as a wide temperature range, different initial temperatures encountered, and differing gradients that they are expected to experience in the soil in different climates (Yamada and Ohshima, 2003; Anderson et al., 2007; Ramot et al., 2008b; Nakazato and Mochizuki, 2009; Jurado et al., 2010). Thus, this behavior has evolved to be both robust and highly flexible.

The sensory neurons required for negative thermotaxis have been partly elucidated. The bilateral AFD neurons are a major thermosensory neuron type in *C. elegans* (Mori and Ohshima, 1995), and exhibit temperature-induced changes in activity at temperatures above T_c (Kimura et al., 2004; Clark et al., 2006; Ramot et al., 2008a). The threshold of temperature responses in

Received March 2, 2011; revised May 26, 2011; accepted June 21, 2011.

Author contributions: M.B. and P.S. designed research; M.B. and S.A. performed research; M.B. and P.S. analyzed data; P.S. wrote the paper.

This work was supported in part by the NIH (R01 GM081639 to P.S., Core Grant P30 NS45713 to the Brandeis Biology Department, T32 EB009419 to M.B.) and the National Science Foundation (Integrative Graduate Education and Research Traineeship Program DGE-0549390 to M.B.). We are grateful to Harry Bell for technical assistance, Cori Bargmann, Miriam Goodman, and Kyuhyung Kim for reagents, and Cori Bargmann, David Biron, Eve Marder, Miriam Goodman, Sara Wasserman, and the Sengupta laboratory for critical comments and advice.

Correspondence should be addressed to Piali Sengupta at the above address. E-mail: sengupta@brandeis.edu.

DOI:10.1523/JNEUROSCI.1098-11.2011

 0270-6474/11/3111718-10$15.00/0

AFD is determined by T_c (Kimura et al., 2004; Biron et al., 2006; Clark et al., 2006; Ramot et al., 2008a), and provides a cellular correlate for T_c memory. In addition to AFD, the AWC sensory neurons also respond to temperature in a T_c-dependent manner and modulate negative thermotaxis (Biron et al., 2008; Kuhara et al., 2008). However, the roles of AFD and AWC in generating thermotactic navigation behaviors have been examined only under a limited set of conditions. Thus, how these neurons contribute to thermosensory behaviors under different conditions and whether additional neurons are also required are unknown.

Here we show that the strategy underlying negative thermotaxis behavior is generated via different configurations of thermosensory neurons under conditions of varying T_c and temperature range of the thermal gradient. We identify the ASI chemosensory neurons as a new component of the thermosensory circuit, and show that this neuron type responds to temperature changes within a T_c-dependent operating range. Interestingly, we find that AFD may set the operating range of ASI under specific conditions via peptidergic neuromodulation. Our observations describe a mechanism that may buffer the network from genetic or physical perturbation, and allow animals to mount a robust and coherent behavioral response over a wide range of environmental conditions.

Materials and Methods

Strains. The wild-type strain was *C. elegans* Bristol, strain N2, raised on OP50 bacterial lawns. Mutant strains used were PR678 *tax-4*(*p678*); KR1787 *unc-13*(*e51*); CB169 *unc-31*(*e169*); and GN112 [*pgIs1* (AFD-ablated); gift from Miriam Goodman, Stanford University, Palo Alto, CA] (Glauser et al., 2011).

The AWC-ablated strain (PY7502) was generated via expression of recCaspases (Chelur and Chalfie, 2007) under *ceh-36* (Kim et al., 2010) promoter sequences together with *gfp* driven under the *srtx-1* promoter (Colosimo et al., 2004) to visualize loss of AWC. The *ceh-36* regulatory sequences used drive expression exclusively in the AWC neurons (Kim et al., 2010). Loss of AWC neurons was confirmed by the absence of *gfp* expression driven under the *srtx-1* promoter and failure of AWC-ablated animals to respond to an AWC-sensed odorant (Bargmann et al., 1993). The ASI-ablated strain (PY7505) was generated via expression of recCaspases under the *gpa-4* (Jansen et al., 1999) and *gcy-27* (Ortiz et al., 2006) promoters together with *gfp* expression under the *gcy-27* promoter to confirm loss of ASI. Loss of ASI neurons was also confirmed by failure of the ASI neurons to uptake a lipophilic dye (Herman and Hedgecock, 1990), and constitutive entry of ASI-ablated animals into the alternate dauer developmental stage (Bargmann and Horvitz, 1991; Ailion and Thomas, 2000). A fraction of ASI-ablated animals bypassed the dauer stage and grew into adults, allowing examination of their thermosensory behavioral phenotypes. recCaspase-expressing constructs were injected at 50 ng/μl. Extrachromosomal arrays carrying the recCaspase constructs and cell-specific markers were stably integrated into the genome via UV irradiation-induced mutagenesis, and outcrossed at least twice before analyses. Strains lacking two neuron types were generated by crossing together strains lacking each individual cell type.

Strains expressing wild-type *tax-4* cDNA in specific cell types were generated by injecting the expression construct at 20 ng/μl with the *unc-122*p::dsRed coinjection marker at 50 ng/μl. At least two independent transgenic lines were generated for each construct and exhibited similar behaviors. For strains expressing *tax-4* in multiple cell types, constructs driving expression in individual cell types were coinjected. Constructs driving *pkc-1*(*gf*) expression were injected at 50 ng/μl together with a coinjection marker. Corresponding wild-type and AFD-ablated strains shown in Figure 3*F* carried the same extrachromosomal arrays expressing *pkc-1*(*gf*).

Molecular biology. Wild-type *tax-4* cDNA sequences (Satterlee et al., 2004) were expressed under the following promoters: *ttx-1* (AFD) (Satterlee et al., 2001), *ceh-36* (AWC) (Kim et al., 2010), *srbc-65* (ASI) (Kim et al., 2009), *osm-10* (ASH, ASI, PHA, PHB) (Hart et al., 1999), *ops-1* (ASG) (Sarafi-Reinach and Sengupta, 2000). Promoters driving recCaspase expression were as follows: *ceh-36* (AWC) (Chelur and Chalfie, 2007), *gpa-4* and *gcy-27* (ASI) (Jansen et al., 1999), *str-3* and *gpa-4* [ASI (EC1)] (Jansen et al., 1999; Peckol et al., 2001), *gcy-27* and *str-3* [ASI (EC2)] (Peckol et al., 2001), *srtx-1* [AFD and AWC (EC1)] (Colosimo et al., 2004). The *pkc-1*(*gf*) cDNA was expressed under the following promoters: *gcy-8* (AFD) (Yu et al., 1997), *ceh-36* (AWC) (Kim et al., 2010), and *srbc-65* (ASI) (Kim et al., 2009). *GCaMP 2.2b* was expressed under the *gpa-4* promoter (courtesy of K. Kim, Brandeis University, Waltham, MA; and C. Bargmann, The Rockefeller University, New York, NY). Constructs were generated in *C. elegans* expression vectors (gift from A. Fire) or using the Gateway system (Invitrogen).

Negative thermotaxis behavioral assays. Assays were performed essentially as previously described (Chi et al., 2007; Clark et al., 2007; Biron et al., 2008). Worms were cultivated overnight with food at the desired T_c. Before the assay, 15 young adult animals were briefly transferred onto a 6 cm NGM plate without food, and then transferred onto the center of a 10 cm agar plate and placed on an aluminum plate. A linear temperature gradient was generated and monitored on the aluminum plate by Peltier thermoelectric temperature controllers (Oven Industries). The temperature of the agar on the assay plate was measured using a two probe digital thermometer (Fluke Electronics) to confirm accuracy. Animals were allowed to move freely for 5 min before the start of the assay. Worm movement was then recorded using a CCD camera (Panasonic WV-CP484) for 30 min with images acquired at 1 Hz. The center of mass for each animal was tracked in each frame by thresholding. Centers of mass were considered particles and individual particles were tracked over time to reflect worm trajectories. Images were analyzed using LabView (National Instruments) and custom-written scripts in MATLAB (The MathWorks). Forward movement of duration >6 s (1 body length) were considered runs. Run trajectories were analyzed with respect to gradient direction. Turns were defined as changes in direction that were >13°/s. Runs that contributed to the negative thermotaxis bias were within 45–315° or 135–225°.

Calcium imaging. Imaging of temperature-evoked Ca^{2+} dynamics in ASI were performed as previously described (Biron et al., 2008). Briefly, animals expressing *GCaMP 2.2b* in ASI were cultivated overnight at a given temperature. Before the start of the assay, individual animals were glued to an agarose pad using cyanoacrylate glue at room temperature. The agarose pad containing the worm was transferred to an indium tin oxide covered slide with 5 μl of water between the pad and slide to ensure good thermal contact. Current controlled via temperature-regulated feedback using LabView was passed through the slide to generate heat, and temperature was measured using a T-type thermocouple. The elapsed time from removal of the animal from the incubator to initiation of imaging was <3 min. Individual animals were imaged for 15 min with upward or downward ramp stimuli and 5 min at constant temperatures at a rate of 2 Hz. Images were captured using MetaMorph (Molecular Devices) and a Hamamatsu Orca digital camera. Data were analyzed using scripts in MATLAB. A fluorescence change >10% in ASI was considered a response.

Results

The TAX-4 cyclic nucleotide-gated channel is required for robust negative thermotaxis bias under multiple growth and assay conditions

Wild-type adult *C. elegans* hermaphrodites exhibit strong negative thermotaxis when grown at different temperatures and placed on thermal gradients at temperatures above T_c (Hedgecock and Russell, 1975; Mori and Ohshima, 1995). To establish a baseline for our assays, we examined negative thermotaxis behaviors of wild-type animals grown at either 15°C or 20°C and placed at temperatures 4–10°C above T_c (T_{start}) in the center of a linear thermal gradient on a 10 cm agar plate (Fig. 1*A*). Since gradient steepness was maintained at 1.0°C/cm, the range of the gradient varied as a function of T_c and T_{start} (Fig. 1*A*). We specifically excluded starting temperatures that were below T_c + 4°C since *C.*

elegans tracks isotherms near T_c (Hedgecock and Russell, 1975; Mori and Ohshima, 1995), and exhibition of this alternate behavior affects negative thermotaxis.

The net displacement of animals on a spatial thermal gradient over time has been used as a measure of negative thermotaxis behavior (Hedgecock and Russell, 1975; Inada et al., 2006; Ramot et al., 2008b). However, since multiple behavioral parameters can contribute to these endpoint accumulations, we focused specifically on quantifying the underlying thermotactic navigational strategy (Ryu and Samuel, 2002; Zariwala et al., 2003; Clark et al., 2007). Detailed measurements of individual animal trajectories have shown that *C. elegans* executes negative thermotaxis using a biased random walk strategy such that forward movement (called runs) is lengthened when animals are moving toward favorable (colder) conditions, and shortened when they are moving toward warmer conditions (Ryu and Samuel, 2002; Zariwala et al., 2003). Runs are terminated by reversals and turns, which reorient the animal in a random direction.

This navigational strategy can be quantified by calculating the thermotaxis bias [similar to the previously described cryophilic bias (Chi et al., 2007; Clark et al., 2007)], which we define as the (total duration of runs in the warmer direction) − (total duration of runs in the colder direction)/total duration of runs. Thus, a negative thermotaxis bias would enable animals to perform negative thermotaxis. Under our conditions, we found that wild-type animals grown at either 15°C or 20°C exhibited a robust negative thermotaxis bias at $T_{start} > T_c + 5$°C (Fig. 1*B*,*C*). This bias was weakened when $T_{start} > T_c + 9$°C for animals grown at 15°C (Fig. 1*B*), although a similar decline was not observed for animals grown at 20°C (Fig. 1*C*), possibly due to activation of nociceptive pathways at higher temperatures (Wittenburg and Baumeister, 1999; Chatzigeorgiou et al., 2010; Glauser et al., 2011). These results are consistent with but not identical to previous observations (Ramot et al., 2008b), likely due to differences in assay parameters and analyses of endpoint measurements as compared to navigational decisions (see Materials and Methods).

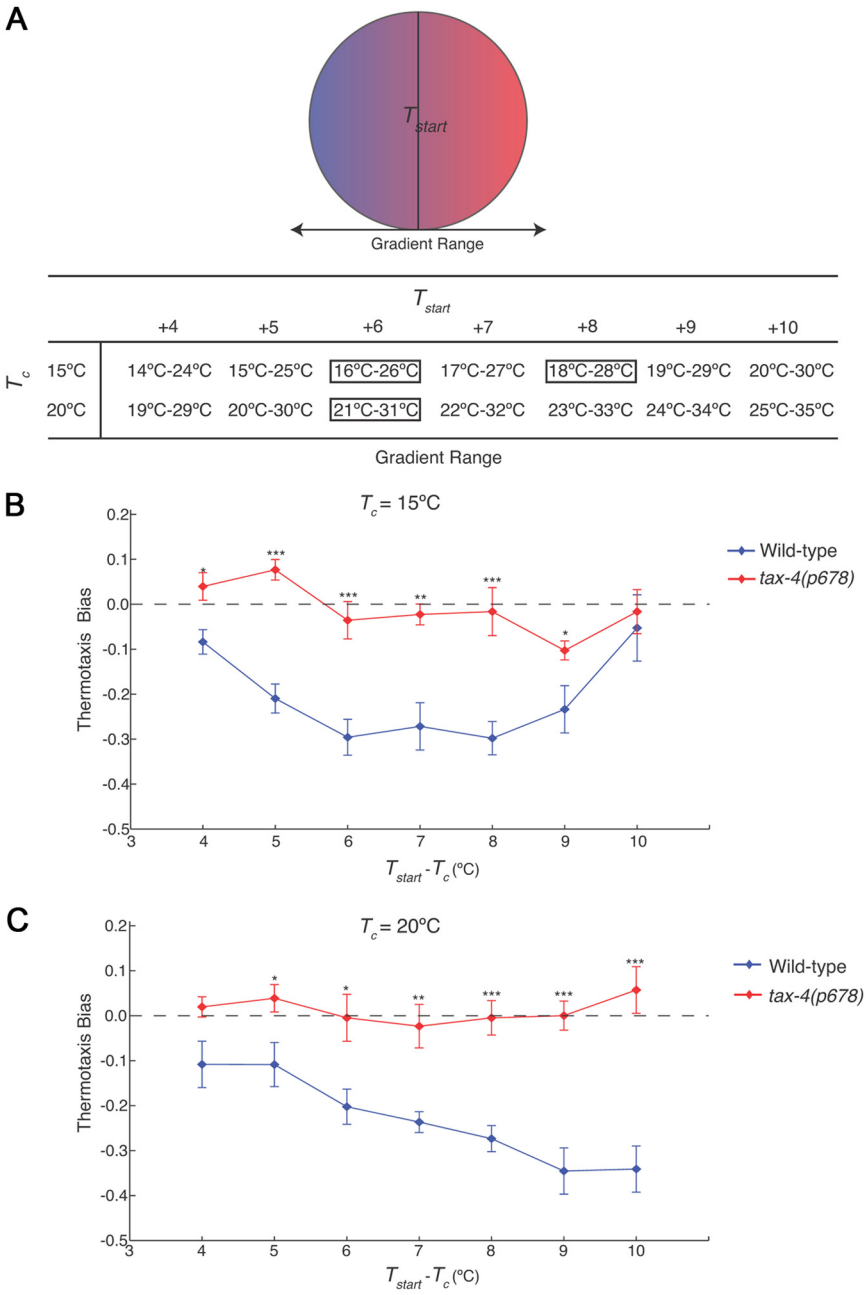

Figure 1. *C. elegans* exhibits robust negative thermotaxis bias under varying conditions. ***A***, Diagram of assay conditions. Gradient steepness was maintained at 1.0°C/cm. Animals were placed in the middle of the gradient at the start of the assay (T_{start}). The temperature ranges of the gradient for varying cultivation temperatures (T_c) and T_{start} are shown. Conditions examined further in this study are boxed. ***B***, ***C***, Thermotaxis bias (see text) exhibited by wild-type and *tax-4*(*p678*) animals for $T_c = 15$°C (***B***) or $T_c = 20$°C (***C***) with varying T_{start}. For each data point, $n = 105$ animals; 7 independent assays. Error bars are the SEM. *, **, and *** indicate significant differences from wild-type values at $p < 0.05$, $p < 0.01$, and $p < 0.001$, respectively, by one-way ANOVA.

The TAX-4 cyclic nucleotide-gated (CNG) channel is expressed in a subset of sensory neurons including the AFD and AWC thermosensory neurons (Komatsu et al., 1996), and is required for thermotactic behaviors under the subset of conditions that have been examined (Mori and Ohshima, 1995; Komatsu et al., 1996). *tax-4* mutants are atactic and fail to exhibit temperature-evoked activity in the AFD thermosensory neurons (Mori and Ohshima, 1995; Kimura et al., 2004; Ramot et al., 2008a). We determined whether TAX-4 is essential for negative thermotaxis under different assay conditions. As shown in Figure 1, *B* and *C*, *tax-4* mutants were atactic regardless of T_c or T_{start}. Thus, wild-type *C. elegans* exhibits a robust negative thermotaxis bias under varying conditions, and this behavior is TAX-4 dependent.

The ASI chemosensory neurons act partly degenerately with the AFD and AWC thermosensory neurons to generate negative thermotaxis bias under specific conditions

We next determined whether known thermosensory neurons contribute in a similar manner to negative thermotaxis behavior

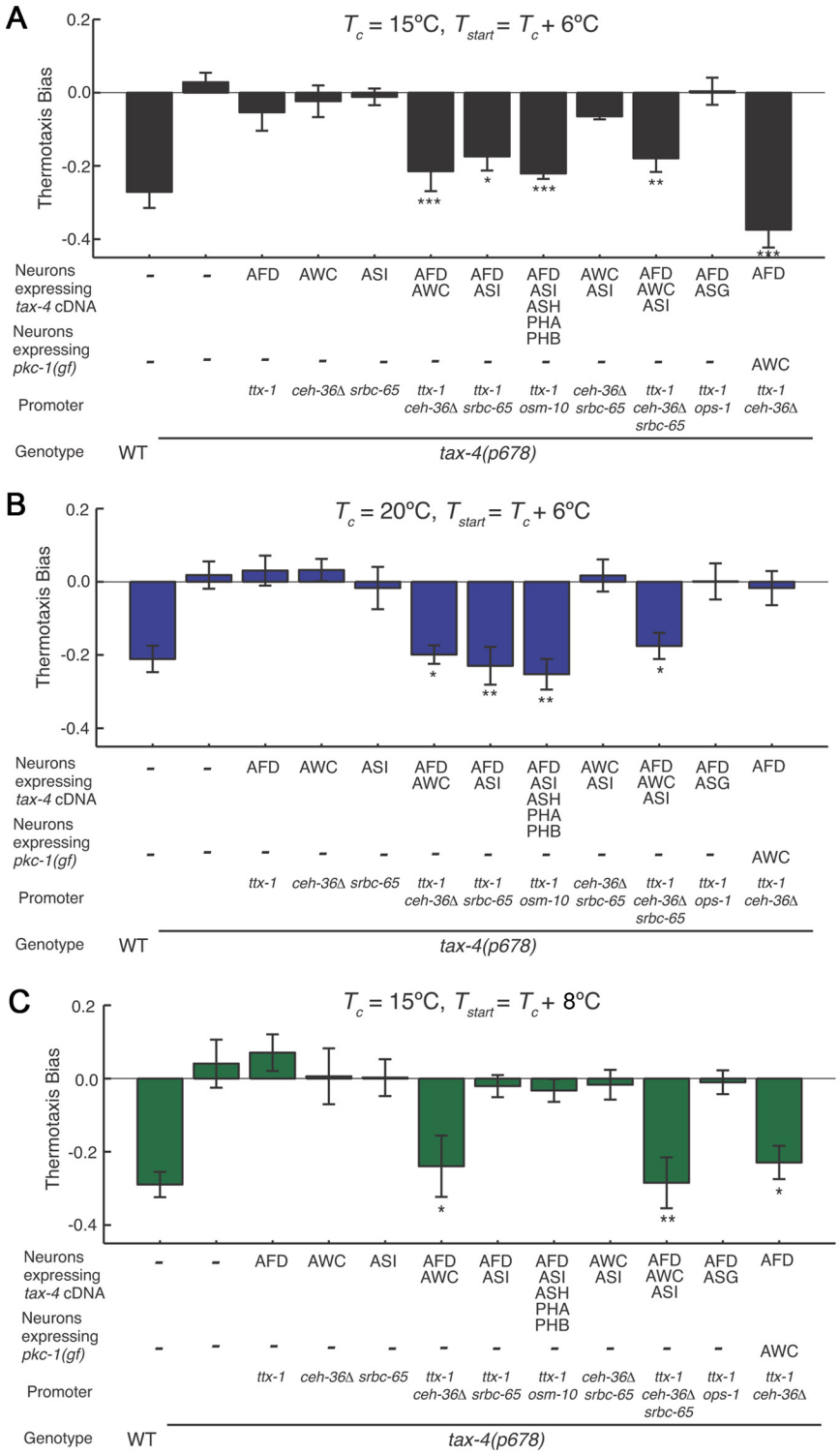

Figure 2. Different sensory neuron subsets are sufficient to restore negative thermotaxis bias to *tax-4* mutants under different conditions. ***A–C***, Thermotaxis bias of transgenic *tax-4*(*p678*) mutants expressing wild-type *tax-4* cDNA under the indicated cell-specific promoters (also see Materials and Methods). Conditions for each assay are indicated above each panel. Values shown are from one transgenic line for each construct; additional transgenic lines showed similar behaviors. For each data point, $n = 105$ animals; 7 independent assays. *, **, and *** indicate significant differences from *tax-4* values at $p < 0.05$, $p < 0.01$, and $p < 0.001$, respectively, by one-way ANOVA with Bonferroni *post hoc* correction. Error bars are the SEM.

under different conditions, or whether additional neurons are recruited under specific circumstances. To address this issue, we restored TAX-4 function to individual *tax-4*-expressing sensory neurons via expression of wild-type *tax-4* sequences under cell-specific or -selective promoters, and quantified thermotaxis bias. Since it was impractical to examine all conditions shown in Figure 1, *B* and *C*, we restricted our analysis to conditions where $T_{start} = T_c + 6$°C or 8°C for $T_c = 15$°C, and $T_c + 6$°C for $T_c = 20$°C. Wild-type animals exhibit a robust negative thermotaxis bias under all these conditions; we elected to not examine higher starting temperatures for animals grown at 20°C to restrict our analysis to non-nociceptive conditions.

We found that restoration of *tax-4* expression to either the known AFD or AWC thermosensory neurons alone did not rescue the *tax-4* thermosensory behavioral defects under any condition (Fig. 2*A–C*), although expression in AWC rescued the defects in AWC-mediated olfactory behaviors (Bargmann et al., 1993) (data not shown). However, expression in both AFD and AWC restored negative thermotaxis bias to levels similar to those exhibited by wild-type animals (Fig. 2*A–C*), indicating that AFD and AWC together are sufficient to confer negative thermotaxis bias under all examined conditions.

We next investigated whether additional *tax-4*-expressing neurons contribute in a degenerate manner with AFD or AWC to maintain behavioral robustness. We were particularly interested in the ASI chemosensory neurons, since gene expression in ASI has previously been shown to be regulated by temperature (Schackwitz et al., 1996; Ailion and Thomas, 2000) similar to the case in AFD (Satterlee et al., 2004), and ASI is presynaptic to interneurons implicated in the thermosensory circuit (White et al., 1986; Mori and Ohshima, 1995). Unexpectedly, we found that restoration of *tax-4* expression in AFD and ASI was sufficient to restore negative thermotaxis bias when $T_{start} = T_c + 6$°C, regardless of T_c (Fig. 2*A*,*B*). However, no rescue was observed upon expression in AFD and ASI when $T_{start} = T_c + 8$°C (Fig. 2*C*). We did not observe behavioral rescue upon expression in AFD and the *tax-4*-expressing ASG chemosensory neurons (Fig. 2*A–C*), upon expression in ASI alone, or together in AWC and ASI under any examined condition (Fig. 2*A–C*). Together, these results indicate that AFD together with either AWC or ASI is sufficient to confer negative thermotaxis bias when $T_{start} = T_c + 6$°C in a *tax-4* mutant background, but that ASI may not contribute at starting temperatures that are distant from T_c.

It is important to note that while expression of wild-type *tax-4* sequences in subsets of these sensory neurons restored the cumulative negative thermotaxis bias under specific conditions, not all

Table 1. Ratio of run durations in the cold and warm directions as a function of time

Strain (neurons expressing wild-type *tax-4* sequences)	$T_c = 15°C, T_{start} + 6°C$			$T_c = 20°C, T_{start} + 6°C$			$T_c = 15°C, T_{start} + 8°C$		
	1st 10 min	2nd 10 min	3rd 10 min	1st 10 min	2nd 10 min	3rd 10 min	1st 10 min	2nd 10 min	3rd 10 min
Wild-type	1.87 ± 0.05$^{\#\#\#}$	1.57 ± 0.07$^{\#\#\#}$	1.15 ± 0.09$^{\#}$	1.54 ± 0.06$^{\#\#\#}$	1.35 ± 0.09$^{\#\#}$	1.19 ± 0.11$^{\#}$	1.73 ± 0.06$^{\#\#\#}$	1.53 ± 0.11$^{\#\#}$	1.61 ± 0.14$^{\#\#}$
tax-4	0.98 ± 0.04***	0.90 ± 0.06***	0.88 ± 0.06*	0.96 ± 0.05***	0.92 ± 0.06**	0.88 ± 0.06*	1.01 ± 0.05***	1.04 ± 0.06**	0.86 ± 0.08**
tax-4 (AFD)	1.12 ± 0.05***	1.02 ± 0.07***	1.05 ± 0.06$^{\#}$	0.89 ± 0.06***	0.94 ± 0.07**	1.09 ± 0.08$^{\#}$	1.02 ± 0.07***	0.84 ± 0.09***$^{\#}$	0.71 ± 0.09***
tax-4 (AWC)	0.92 ± 0.06***	1.08 ± 0.08***	0.94 ± 0.08	1.05 ± 0.07***	0.84 ± 0.08***	0.95 ± 0.09	0.93 ± 0.08***	1.02 ± 0.11**	1.00 ± 0.14*
tax-4 (ASI)	1.10 ± 0.05***	0.87 ± 0.07***	0.92 ± 0.08	1.11 ± 0.10**	0.90 ± 0.09**	0.88 ± 0.12	1.00 ± 0.06***	1.06 ± 0.08*	0.94 ± 0.12**
tax-4 (AFD AWC)	1.37 ± 0.06***$^{\#\#\#}$	1.70 ± 0.09$^{\#\#\#}$	1.11 ± 0.10	1.41 ± 0.07$^{\#\#\#}$	1.70 ± 0.12$^{\#\#\#}$	1.10 ± 0.09	1.34 ± 0.08*$^{\#\#}$	1.50 ± 0.08$^{\#\#}$	1.96 ± 0.10$^{\#\#\#}$
tax-4 (AFD ASI)	1.24 ± 0.06***$^{\#\#}$	1.41 ± 0.08$^{\#\#\#}$	1.15 ± 0.09$^{\#}$	1.50 ± 0.05$^{\#\#\#}$	1.25 ± 0.08$^{\#\#}$	1.11 ± 0.08$^{\#}$	1.03 ± 0.05***	0.97 ± 0.07**	1.09 ± 0.09*
tax-4 (AFD ASI ASH PHA PHB)	1.52 ± 0.07*$^{\#\#\#}$	1.33 ± 0.08$^{\#\#\#}$	1.68 ± 0.09**$^{\#\#\#}$	1.63 ± 0.08$^{\#\#\#}$	1.27 ± 0.09$^{\#\#}$	1.35 ± 0.12$^{\#\#}$	1.29 ± 0.09**$^{\#}$	1.17 ± 0.12	0.72 ± 0.12***
tax-4 (AWC ASI)	1.05 ± 0.06***	1.08 ± 0.06***$^{\#}$	1.13 ± 0.07$^{\#\#}$	1.00 ± 0.09***	0.70 ± 0.11***$^{\#}$	1.12 ± 0.09$^{\#}$	0.87 ± 0.07***	1.22 ± 0.09	1.10 ± 0.08*$^{\#}$
tax-4 (AFD AWC ASI)	1.24 ± 0.06***$^{\#\#}$	1.56 ± 0.08$^{\#\#\#}$	1.13 ± 0.08$^{\#}$	1.44 ± 0.12$^{\#\#}$	1.57 ± 0.11$^{\#\#\#}$	1.03 ± 0.10	1.52 ± 0.08$^{\#\#\#}$	1.41 ± 0.11$^{\#}$	1.23 ± 0.12$^{\#}$
tax-4 (AFD ASG)	1.07 ± 0.06***	0.85 ± 0.06***	0.82 ± 0.08**	1.10 ± 0.07***	0.94 ± 0.09**	1.03 ± 0.08	1.11 ± 0.07***	1.04 ± 0.10*	0.87 ± 0.10**

Ratios ± SEM of run durations in the cold and warm directions averaged in 10 min bins are shown for each strain. *, **, and *** indicate values that are different at $p < 0.05$, 0.01, and 0.001, respectively, from wild-type values. #, ##, and ### indicate values that are different at $p < 0.05$, 0.01, and 0.001, respectively, from *tax-4* values. Data are from Figure 2.

aspects of the overall behavior were fully rescued. Thus, individual strains exhibited differences in the duration of runs toward the cold and warm directions as a function of time when compared to wild-type animals and to each other (Table 1). Thus, while TAX-4 function in subsets of AFD, AWC, or ASI neurons is sufficient to rescue the ability of *tax-4* mutants to modulate their navigation in response to temperature changes, it is likely that additional *tax-4*-expressing neurons also contribute to the overall behavior, further highlighting the importance of dissecting underlying strategies when examining the execution of a behavior.

Since ASI is presynaptic to AWC (White et al., 1986), we next investigated the possibility that restoration of TAX-4 function in ASI activates AWC in the *tax-4* mutant background to generate negative thermotaxis bias. We reasoned that if this is the case, then the behaviors of *tax-4* mutants in which TAX-4 function is restored in AFD and ASI should resemble those of *tax-4* mutant animals in which TAX-4 function is restored only in AFD and in which AWC is activated via cell-specific expression of a constitutively activated allele of the *pkc-1* protein kinase C gene (*pkc-1*(*gf*)). *pkc-1*(*gf*) has been shown to activate neurons likely via promotion of synaptic transmission and neuropeptide release (Okochi et al., 2005; Sieburth et al., 2005, 2007; Tsunozaki et al., 2008; Macosko et al., 2009) (also see Fig. 3*F*). However, the behaviors of animals from these two strains were distinct (Fig. 2*A–C*), suggesting that ASI does not act solely via activation of AWC.

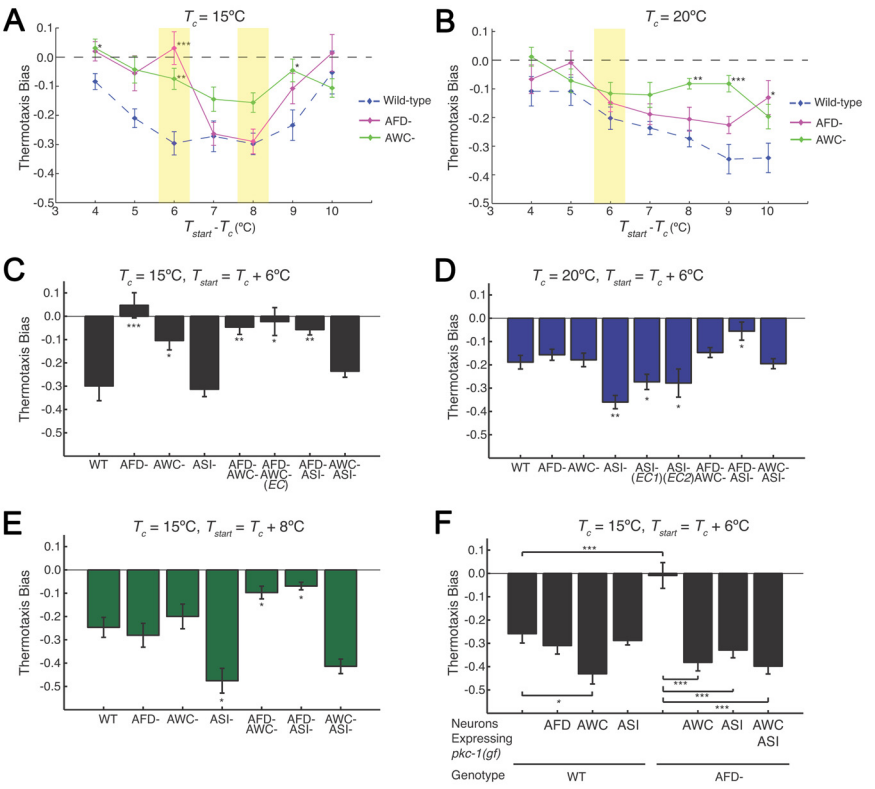

Figure 3. The AFD, AWC, and ASI neurons are required in a degenerate manner to generate negative thermotaxis bias under different conditions. ***A***, ***B***, Thermotaxis bias of wild-type and neuron-ablated strains (see Materials and Methods) under the indicated conditions. Wild-type data from Figure 1 are included for comparison. Data from wild-type, *tax-4*, and neuron-ablated strains shown in Figures 1*B*, 1*C*, 3*A*, and 3*B* were obtained together on multiple days. For each data point, $n = 105$ animals; 7 independent assays. *, **, and *** indicate significant differences from wild-type values at $p < 0.05$, $p < 0.01$, and $p < 0.001$, respectively, by one-way ANOVA with Bonferroni *post hoc* correction. Conditions examined further are shaded. ***C–E***, Thermotaxis bias of indicated strains under the specified conditions. *EC* indicates that the promoter::caspase constructs were driven under different promoter combinations and present as extrachromosomal arrays (see Materials and Methods). $n = 105$ animals; 7 independent assays. *, **, and *** indicate significant differences from wild-type values at $p < 0.05$, $p < 0.01$, and $p < 0.001$, respectively, by one-way ANOVA with Bonferroni *post hoc* correction. Error bars are the SEM. Average speeds (in millimeters per second) of strains were as follows: (T_c = 15°C) wild-type—0.17 ± 0.008, AFD-ablated—0.13 ± 0.002, AWC-ablated—0.17 ± 0.007, ASI-ablated—0.15 ± 0.005; (T_c = 20°C) wild-type—0.18 ± 0.005, AFD-ablated—0.14 ± 0.004, AWC-ablated—0.20 ± 0.003, ASI-ablated—0.15 ± 0.004. ***F***, Thermotaxis bias of wild-type or AFD-ablated strains expressing *pkc-1*(*gf*) under cell-specific promoters from extrachromosomal arrays. Numbers shown are from one transgenic line each. $n = 105$ animals; 7 independent assays. * and *** indicate significant differences at $p < 0.05$ and $p < 0.001$, respectively, between values indicated by brackets (one-way ANOVA with Bonferroni *post hoc* correction). Error bars are the SEM.

Different subsets of sensory neurons are necessary for negative thermotaxis bias under distinct conditions

The above experiments established sufficiency of subsets of sensory neurons to generate negative thermotaxis bias under different conditions in a *tax-4* mutant background; we next investigated their necessity. We generated strains in which each of the AWC or ASI neurons has been genetically ablated via cell-specific expression of caspases in an otherwise wild-type background (see Materials and Methods) (Chelur and Chalfie, 2007). A strain in

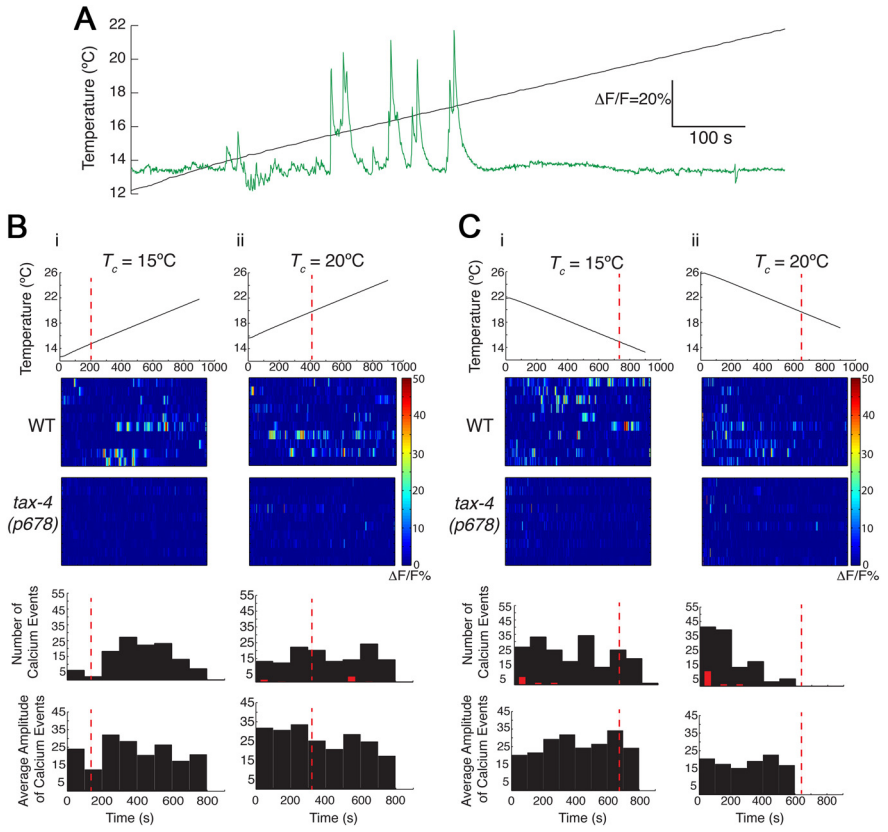

Figure 4. The ASI neurons exhibit intracellular changes in Ca^{2+} dynamics in response to temperature changes. ***A***, Representative example of a rising temperature stimulus (black) and Ca^{2+} events (green) in an ASI neuron expressing *GCaMP 2.2*. T_c = 15°C. ***B***, ***C***, Heat maps and histograms showing responses of individual ASI neurons in wild-type or *tax-4* mutants to a linear upward (***B***) or downward (***C***) temperature ramp at the indicated T_c. The slope of the ramps was 0.01°C/s. Each line in the heat maps represents the responses of one neuron. Red dotted lines indicate T_c. Red bars indicate number of observed Ca^{2+} events in *tax-4* mutants; responses are different at $p < 0.001$ (***Bi***) and $p < 0.01$ (***Bii***, ***Ci***, ***Cii***) compared to wild-type values using a Kruskal–Wallis nonparametric test. Amplitudes of events in *tax-4* mutants are not shown. A fluorescence change of >10% was considered a response. $n = 10$ neurons each.

which the AFD neurons have been similarly ablated via expression of a caspase has been reported (Glauser et al., 2011). We confirmed that ablation of each of the AFD, AWC, and ASI neurons did not significantly affect overall speed at either T_c = 15°C or T_c = 20°C (legend to Fig. 3).

We first determined the requirement for each of the previously identified AWC and AFD thermosensory neurons in the generation of negative thermotaxis bias under conditions of varying T_c and T_{start}. Surprisingly, we found that ablation of AFD or AWC resulted in significant defects in negative thermotaxis bias only under a limited set of examined conditions (Fig. 3*A*,*B*). Thus, loss of AFD alone abolished the negative bias at T_c = 15°C and $T_{start} = T_c$ + 6°C (Fig. 3*A*,*C*), but had little effect under other examined conditions (Fig. 3*A*–*E*). Ablation of AWC also significantly decreased negative thermotaxis bias at T_c = 15°C and $T_{start} = T_c$ + 6°C (Fig. 3*A*,*C*), as well as at higher temperatures relative to T_c (Fig. 3*A*,*B*), but had little effect under other conditions (Fig. 3*A*–*E*).

We next determined whether multiple thermosensory neurons are necessary to confer negative thermotaxis bias under specific conditions. We found that while ablation of both AFD and AWC resulted in a lack of any bias when T_c = 15°C regardless of T_{start} (Fig. 3*C*,*E*), no effects were observed at T_c = 20°C (Fig. 3*D*). In contrast, ablation of both AFD and ASI abolished negative thermotaxis bias under all conditions (Fig. 3*C*–*E*). Loss of ASI alone resulted in enhanced negative thermotaxis bias under a subset of conditions (Fig. 3*D*,*E*). It is likely that additional compensatory mechanisms contribute to this behavior, since we found that loss of AWC and ASI restored negative thermotaxis bias at T_c = 15°C and $T_{start} = T_c$ + 6°C (Fig. 3*C*). The cell specificity of the ablations were verified by examining the behaviors of strains in which one or more of these neurons were ablated via caspase expression under independent promoters ("EC," Fig. 3*C*,*D*). Together, these results indicate that different sensory neuron combinations are necessary to generate negative thermotaxis bias under different conditions.

The contributions of sensory neurons to negative thermotaxis bias can be altered by enhancing their output

The above data indicate that at T_c = 15°C and $T_{start} = T_c$ + 6°C, ablation of AFD strongly decreases negative thermotaxis bias (Fig. 3*A*,*C*). Since AWC and ASI act partly redundantly under other conditions together with AFD (Fig. 3*D*,*E*), we investigated whether activation of one or both of these neuron types would be sufficient to bypass the effects of AFD loss under these conditions.

Expression of *pkc-1(gf)* in either AFD or ASI in an otherwise wild-type background did not affect negative thermotaxis bias (Fig. 3*F*), although expression in AWC weakly enhanced the bias (Fig. 3*F*). However, *pkc-1(gf)* expression in either AWC or ASI in an AFD-ablated background was sufficient to fully bypass the behavioral defects and restore negative thermotaxis bias (Fig. 3*F*). Expression of *pkc-1(gf)* in both AWC and ASI did not further enhance the behavioral phenotype (Fig. 3*F*). These results indicate that activation of either AWC or ASI output can bypass loss of AFD function under the conditions examined, further supporting the hypothesis that these neurons can act degenerately to generate negative thermotaxis bias.

The ASI neurons respond to temperature within a T_c-defined operating range

Since a role for the ASI chemosensory neurons in regulating thermosensory behaviors has not been described previously, we next investigated whether ASI responds to temperature by expressing the genetically encoded Ca^{2+} sensor *GCaMP 2.2b* (Nakai et al., 2001) cell-specifically in ASI and monitoring intracellular Ca^{2+} dynamics. In response to a linear upward or downward temperature ramp with a slope of 0.01°C/s (Clark et al., 2006), we detected Ca^{2+} transients in the ASI cell bodies. These responses were stochastic and characterized by an average 3 s rise in Ca^{2+} followed by an average 20 s decay back to baseline with varying amplitudes (Fig. 4*A*). Responses were largely observed at temperatures greater than T_c at both T_c = 15°C and 20°C when temperatures were rising or falling, respectively (Fig. 4*Bi*,*Cii*), although responses were also observed at temperatures below T_c under the converse conditions (Fig. 4*Bii*,*Ci*). Response amplitudes did not vary signif-

icantly across the operating ranges (Fig. 4*B*,*C*). We also noted that there may be an upper bound to the response range at T_c = 15°C when temperatures were rising such that fewer responses were observed at higher temperatures (Fig. 4*Bi*). Response frequency was significantly decreased in *tax-4* mutants under all conditions (Fig. 4*B*,*C*) indicating that as in AWC and AFD, ASI thermosensory responses are likely to be mediated via cGMP signaling.

Our behavioral experiments indicate that the contribution of different sensory neurons to negative thermotaxis bias varies with T_{start}. To mimic the conditions encountered by animals when initiating negative thermotaxis and to further examine the operating range of ASI, we grew animals at 15°C or 20°C, and then shifted them to a different temperature immediately before imaging. Consistent with observations in response to an upward linear temperature ramp, we found that for animals grown at T_c = 15°C, Ca^{2+} responses were first observed when shifted to 17°C (Fig. 5*A*,*B*). Response frequency increased when shifted to 19°C, but then decreased when shifted to 21°C and higher (Fig. 5*A*,*B*). Similarly, for animals grown at 20°C, responses were first observed at 20°C with an increase in frequency upon shift to higher temperatures followed by a decrease (Fig. 5*C*,*D*). Thus, when grown at either 15°C or 20°C, highest response frequency was observed when animals were shifted to T_c + 3 to 5°C, with fewer responses at or below T_c as well as at temperatures far from T_c (Fig. 5*B*,*D*). These results indicate that ASI has a defined but plastic operating range whose lower and upper bounds may be defined by T_c.

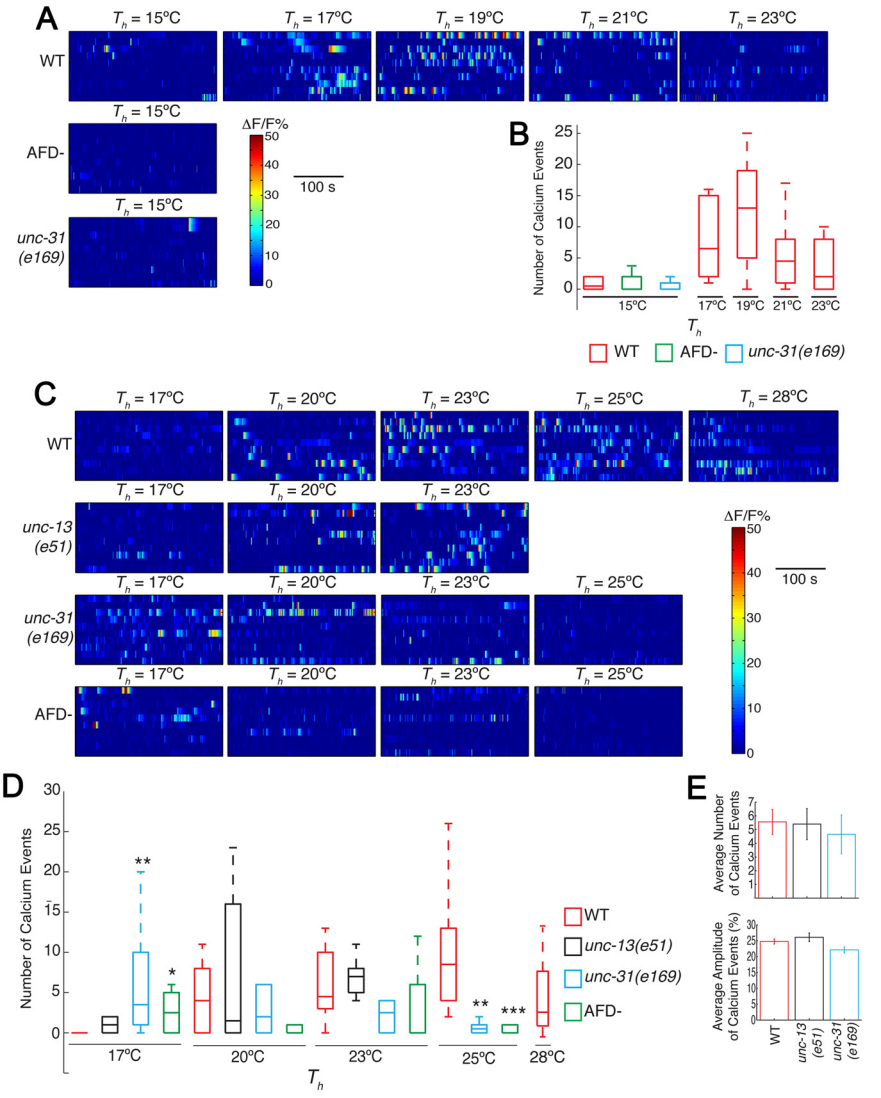

Figure 5. The operating range of ASI may be regulated by AFD-mediated neuromodulation. ***A***, ***C***, Heat maps of responses of individual ASI neurons upon temperature shifts. T_c = 15°C (***A***) or 20°C (***C***). T_h indicates the holding temperature at which responses were quantified. ***B***, ***D***, Box-and-whisker plots of the frequency range of Ca^{2+} events upon temperature shifts to T_h in the indicated genetic backgrounds. For this quantification, a fluorescence change of >10% was considered a response. Boxes indicate the 25th (lower boundary), 50th (median indicated by a line), and 75th (upper boundary) percentiles. Whiskers show the minimum and maximum numbers of events. *, **, and *** indicate values that are different at $p < 0.05$, 0.01, and 0.001, respectively, from the corresponding wild-type values using the Kruskal–Wallis nonparametric test. n = 10 neurons for each data point. ***E***, Average response frequencies and amplitudes of wild-type and *unc-13*(*e51*) and *unc-31*(*e169*) mutants at T_c = 20°C. Averages are calculated from data shown in ***C***.

The operating range of ASI may be partly set by AFD-mediated neuromodulation

Since ASI shares synaptic connections with neurons previously implicated in the thermosensory circuit (White et al., 1986), we next examined whether thermosensory responses of ASI are set via neuromodulation. To examine a role for synaptic transmission, we examined ASI responses in animals carrying the *e51* lesion in the *unc-13* synaptic protein gene; this lesion specifically affects synaptic vesicle exocytosis (Speese et al., 2007). We also examined animals mutant for the *unc-31* CAPS protein gene, which regulates dense core vesicle exocytosis and thus neuropeptidergic signaling, and may also affect synaptic transmission (Ann et al., 1997; Berwin et al., 1998; Renden et al., 2001; Grishanin et al., 2004; Fujita et al., 2007; Sieburth et al., 2007; Speese et al., 2007). The average frequency and amplitude of ASI Ca^{2+} responses were largely unaffected in either mutant background (Fig. 5*E*), implying that ASI may be directly thermosensory, although regulation of ASI responses via electrical synapses cannot be ruled out (Macosko et al., 2009; Chatzigeorgiou and Schafer, 2011). Interestingly however, we found that the operating range of ASI was shifted in *unc-31* but not in *unc-13* mutants in a T_c-dependent manner (Fig. 5*C*,*D*). Thus, in *unc-31* mutants grown at 20°C, a significant number of Ca^{2+} events were observed when animals were shifted to 17°C, with a correlated downward shift in the upper bound of the operating range (Fig. 5*C*,*D*). This shift was evident at T_c = 20°C, but not at T_c = 15°C (compare Fig. 5*B*,*D*), implying a T_c dependence of this signaling.

We next determined whether signaling from AFD plays a role in setting the operating range of ASI. To do so, we examined temperature-induced Ca^{2+} responses in ASI in strains lacking AFD. We found that a significant number of events were also observed at 17°C with a downward shift in the upper bound, similar to observations in *unc-31* mutants (Fig. 5*C*,*D*). The effects of AFD ablations were again evident at T_c = 20°C but not at 15°C

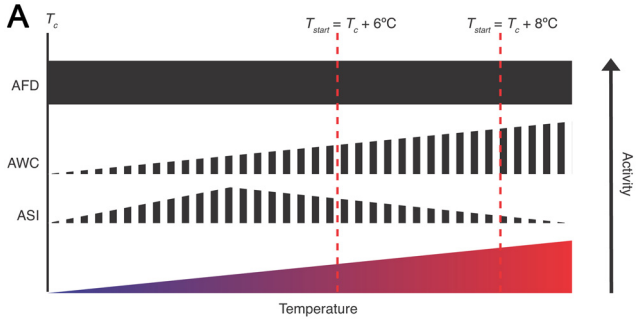

B

	Temperature range of gradient		
	16°C-26°C	18°C-28°C	21°C-31°C
Assay conditions	T_c = 15°C $T_{start} = T_c + 6°C$	T_c = 15°C $T_{start} = T_c + 8°C$	T_c = 20°C $T_{start} = T_c + 6°C$
Necessary	AFD or AWC	AFD+AWC or AFD+ASI	AFD+ASI
Sufficient	AFD+AWC or AFD+ASI	AFD+AWC	AFD+AWC or AFD+ASI

Figure 6. Necessity and sufficiency of distinct subsets of thermosensory neurons under different conditions. ***A***, Shown are the inferred activity levels of AFD, AWC, and ASI at different temperatures above T_c (Kimura et al., 2004; Chung et al., 2006; Biron et al., 2008; Kuhara et al., 2008; Ramot et al., 2008a). Filled and striped boxes indicate deterministic and stochastic Ca^{2+} events in response to temperature, respectively. All temperatures above T_c have not yet been systematically tested for AFD and AWC. ***B***, Neurons shown to be necessary and/or sufficient for negative thermotaxis bias are indicated below for each examined condition and gradient temperature range.

(Fig. 5*B*,*D*). Consistent with the lack of direct synaptic connections from AFD to ASI (White et al., 1986), these results suggest that AFD may signal via neuropeptides to set the operating range of ASI under specific conditions.

Discussion

Our results suggest that degeneracy among thermosensory neurons contributes to the maintenance of behavioral robustness. We identify the ASI chemosensory neurons as new thermosensory components of this circuit, and describe a role for neuromodulation in regulating thermosensory neuron properties. Our findings emphasize the importance of defining conditions when dissecting neuronal contributions to a behavior, and demonstrate that similar behavioral strategies can be driven by different neuron combinations.

Multiple sensory neuron configurations can generate the same behavioral strategy under different conditions

Different combinations of AFD, AWC, and ASI are necessary and sufficient to generate negative thermotaxis bias depending on the environmental context (Fig. 6). It is important to note that the AFD, AWC, and ASI neurons are not structurally or functionally redundant in that each neuron type has independent functions and contributes to generation of the bias and the overall behavior in a unique manner (Bargmann and Horvitz, 1991; Bargmann et al., 1993; Mori and Ohshima, 1995; Ailion and Thomas, 2000; Wagner, 2005; Chung et al., 2006; Biron et al., 2008; Kuhara et al., 2008; Whitacre and Bender, 2010) (Fig. 6*A*). Instead, it is the ability of each of these neuron types to be incorporated into the thermosensory circuit under specific conditions that permits the generation of negative thermotaxis bias over a wide range of environmental parameters. Why specific neuron types are required under specific conditions is not yet clear, although it is intriguing to note that the extent of degeneracy appears to correlate with absolute temperature (Fig. 6*B*). Thus, while loss of any one of two single thermosensory neurons affects the bias at lower temperatures, this behavior is affected only upon loss of one pairwise combination of three thermosensory neurons at the highest temperatures examined (Fig. 6*B*). We speculate that increased degeneracy among thermosensory neurons driving negative thermotaxis at higher temperatures enables increased robustness allowing animals to escape potentially harmful conditions.

Work in multiple systems suggests that degeneracy may be a common property of neuronal networks. For instance, simulation has shown that the same output can be generated by compensatory changes in synaptic strengths and neuronal properties in a simple model circuit (Prinz et al., 2004; Tang et al., 2010), and reconfiguration of contributions of individual neurons under different conditions results in similar motor patterns from the crab gastric mill central pattern generator circuit (Saideman et al., 2007). In *C. elegans*, a distributed circuit contributes to hyperoxia avoidance under different conditions (Chang et al., 2006), and different groups of gustatory neurons are recruited to mediate attraction to salt depending on oxygen concentrations (Pocock and Hobert, 2010). Recent work also indicates that robustness of mating behavior is conferred via a distributed network of ray sensory neurons in the *C. elegans* male (Koo et al., 2011). This flexibility in circuit configuration may greatly enhance the adaptability of the system to constantly changing environmental demands.

Our results also raise the intriguing possibility that many, and perhaps all, *C. elegans* sensory neurons are polymodal. To date, at least five sensory neuron types including ASI, AFD and AWC in *C. elegans* have been shown to respond to multiple sensory stimuli (Bargmann et al., 1993; Hart et al., 1995; Maricq et al., 1995; Biron et al., 2008; Kuhara et al., 2008; Chatzigeorgiou et al., 2010; Bretscher et al., 2011). This multifunctionality may greatly expand the sensory repertoire of an organism with a small number of sensory neurons, and further increases the opportunities for functional degeneracy.

Each thermosensory neuron type responds to temperature in a unique manner

An intriguing feature of the *C. elegans* thermosensory neurons is that each neuron type exhibits cell type-specific responses to temperature changes. Imaging experiments have shown that Ca^{2+} dynamics in AFD to temperature stimuli are deterministic and highly reproducible and are restricted to temperatures above T_c (Kimura et al., 2004; Clark et al., 2006). Although AFD exhibits a restricted operating range for stimuli relevant for isothermal tracking behavior around T_c (Wasserman et al., 2011), the responses of these neurons to temperature changes are similar over the temperature range relevant for negative thermotaxis (Kimura et al., 2004; Clark et al., 2006) (Fig. 6*A*). In contrast, the AWC neurons exhibit stochastic temperature-evoked Ca^{2+} changes that are stimulus-correlated with different temporal kinetics at temperatures above and below T_c (Biron et al., 2008). Moreover, AWC appears to be more active at temperatures further from T_c (Biron et al., 2008) (Fig. 6*A*). Temperature-induced activity in ASI is again distinct; these neurons also exhibit temperature-induced stochastic Ca^{2+} transients in a defined operating range with decreased responses close to or far from T_c (Fig. 6*A*). Regardless of these unique patterns of responses, these neurons are able to partly compensate for loss of other thermosensory neu-

rons under defined conditions (Fig. 6*B*). Moreover, manipulation of neuronal output via expression of *pkc-1*(*gf*) can also bypass the requirement for specific neuron types. Thus, the behavioral output must be an emergent property of the circuit following integration of information from thermosensory neurons. A major next step will be to determine how the circuit compensates for the loss of individual neuron types by comparing activity in shared and unique downstream interneuron and motor neuron subsets in the absence and presence of specific thermosensory neurons.

Neuromodulation may coordinate the operating ranges of multiple thermosensory neurons

Despite exhibiting different temperature response patterns, both AFD and ASI are responsive to temperature changes largely above T_c (Kimura et al., 2004; Clark et al., 2006; this work). Coherence of the T_c-dependent response thresholds between the two neuron types may be regulated via neuropeptidergic signaling from AFD at $T_c = 20$°C. This signaling may serve to ensure that both neurons are functional in the same temperature range relative to T_c. Coherence among network components via neuromodulation has been observed in the circadian network in mammals where nearly all cell types can generate rhythms in a cell-autonomous manner, but whose phases are synchronized in part by hormonal signaling from the "master" oscillator in the suprachiasmatic nucleus (Reppert and Weaver, 2002; Dibner et al., 2010). However, despite the obvious importance of AFD, the thermosensory circuit can still retain functionality in the absence of AFD under certain circumstances, highlighting its distributed nature. It remains possible that signaling within the thermosensory circuit is more complex and may include feedback signaling from shared downstream interneurons to modulate thermosensory neuron properties (Tomioka et al., 2006; Ignell et al., 2009; Chalasani et al., 2010).

Our observations reveal remarkable complexity in the small and hard-wired neuronal network of *C. elegans*. Given the conservation of neuronal functions and circuit properties across species, this work suggests that degenerate components that generate the same behavioral strategy under different conditions may be a common feature of most, if not all nervous systems, and may contribute to the maintenance of critical behaviors under dynamic environmental conditions.

References

Ailion M, Thomas JH (2000) Dauer formation induced by high temperatures in *Caenorhabditis elegans.* Genetics 156:1047–1067.

Anderson JL, Albergotti L, Proulx S, Peden C, Huey RB, Phillips PC (2007) Thermal preference of *Caenorhabditis elegans*: a null model and empirical tests. J Exp Biol 210:3107–3116.

Ann K, Kowalchyk JA, Loyet KM, Martin TF (1997) Novel Ca^{2+}-binding protein (CAPS) related to UNC-31 required for Ca^{2+}-activated exocytosis. J Biol Chem 272:19637–19640.

Bargmann CI, Horvitz HR (1991) Control of larval development by chemosensory neurons in *Caenorhabditis elegans.* Science 251:1243–1246.

Bargmann CI, Hartwieg E, Horvitz HR (1993) Odorant-selective genes and neurons mediate olfaction in *C. elegans.* Cell 74:515–527.

Berwin B, Floor E, Martin TF (1998) CAPS (mammalian UNC-31) protein localizes to membranes involved in dense-core vesicle exocytosis. Neuron 21:137–145.

Biron D, Shibuya M, Gabel C, Wasserman SM, Clark DA, Brown A, Sengupta P, Samuel AD (2006) A diacylglycerol kinase modulates long-term thermotactic behavioral plasticity in *C. elegans.* Nat Neurosci 9:1499–1505.

Biron D, Wasserman S, Thomas JH, Samuel AD, Sengupta P (2008) An olfactory neuron responds stochastically to temperature and modulates *C. elegans* thermotactic behavior. Proc Natl Acad Sci U S A 105: 11002–11007.

Bretscher AJ, Kodama-Namba E, Busch KE, Murphy RJ, Soltesz Z, Laurent P, de Bono M (2011) Temperature, oxygen and salt-sensing neurons in *C. elegans* are carbon dioxide sensors that control avoidance behavior. Neuron 69:1099–1113.

Chalasani SH, Kato S, Albrecht DR, Nakagawa T, Abbott LF, Bargmann CI (2010) Neuropeptide feedback modifies odor-evoked dynamics in *Caenorhabditis* elegans olfactory neurons. Nat Neurosci 13:615–621.

Chang AJ, Chronis N, Karow DS, Marletta MA, Bargmann CI (2006) A distributed chemosensory circuit for oxygen preference in *C. elegans.* PLoS Biol 4:e274.

Chatzigeorgiou M, Schafer WR (2011) Lateral facilitation between primary mechanosensory neurons controls nose touch perception in *C. elegans.* Neuron 70:299–309.

Chatzigeorgiou M, Yoo S, Watson JD, Lee WH, Spencer WC, Kindt KS, Hwang SW, Miller DM 3rd, Treinin M, Driscoll M, Schafer WR (2010) Specific roles for DEG/ENaC and TRP channels in touch and thermosensation in *C. elegans* nociceptors. Nat Neurosci 13:861–868.

Chelur DS, Chalfie M (2007) Targeted cell killing by reconstituted caspases. Proc Natl Acad Sci U S A 104:2283–2288.

Chi CA, Clark DA, Lee S, Biron D, Luo L, Gabel CV, Brown J, Sengupta P, Samuel AD (2007) Temperature and food mediate long-term thermotactic behavioral plasticity by association-independent mechanisms in *C. elegans.* J Exp Biol 210:4043–4052.

Chung SH, Clark DA, Gabel CV, Mazur E, Samuel AD (2006) The role of the AFD neuron in *C. elegans* thermotaxis analyzed using femtosecond laser ablation. BMC Neurosci 7:30.

Clark DA, Biron D, Sengupta P, Samuel ADT (2006) The AFD sensory neurons encode multiple functions underlying thermotactic behavior in *C. elegans.* J Neurosci 26:7444–7451.

Clark DA, Gabel CV, Lee TM, Samuel AD (2007) Short-term adaptation and temporal processing in the cryophilic response of *Caenorhabditis elegans.* J Neurophysiol 97:1903–1910.

Colosimo ME, Brown A, Mukhopadhyay S, Gabel C, Lanjuin AE, Samuel AD, Sengupta P (2004) Identification of thermosensory and olfactory neuron-specific genes via expression profiling of single neuron types. Curr Biol 14:2245–2251.

Dibner C, Schibler U, Albrecht U (2010) The mammalian circadian timing system: organization and coordination of central and peripheral clocks. Annu Rev Physiol 72:517–549.

Edelman GM, Gally JA (2001) Degeneracy and complexity in biological systems. Proc Natl Acad Sci U S A 98:13763–13768.

Fujita Y, Xu A, Xie L, Arunachalam L, Chou TC, Jiang T, Chiew SK, Kourtesis J, Wang L, Gaisano HY, Sugita S (2007) Ca^{2+}-dependent activator protein for secretion 1 is critical for constitutive and regulated exocytosis but not for loading of transmitters into dense core vesicles. J Biol Chem 282:21392–21403.

Glauser DA, Chen WC, Agin R, MacInnis BL, Hellman AB, Garrity PA, Tan MW, Goodman MB (2011) Heat avoidance is regulated by transient receptor potential (TRP) channels and a neuropeptide signaling pathway in *C. elegans.* Genetics 188:91–103.

Golden JW, Riddle DL (1984) The *Caenorhabditis elegans* dauer larva: developmental effects of pheromone, food, and temperature. Dev Biol 102:368–378.

Grishanin RN, Kowalchyk JA, Klenchin VA, Ann K, Earles CA, Chapman ER, Gerona RR, Martin TF (2004) CAPS acts at a prefusion step in dense-core vesicle exocytosis as a PIP2 binding protein. Neuron 43:551–562.

Hart AC, Sims S, Kaplan JM (1995) Synaptic code for sensory modalities revealed by *C. elegans* GLR-1 glutamate receptor. Nature 378:82–85.

Hart AC, Kass J, Shapiro JE, Kaplan JM (1999) Distinct signaling pathways mediate touch and osmosensory responses in a polymodal sensory neuron. J Neurosci 19:1952–1958.

Hartman JL 4th, Garvik B, Hartwell L (2001) Principles for the buffering of genetic variation. Science 291:1001–1004.

Hedgecock EM, Russell RL (1975) Normal and mutant thermotaxis in the nematode *Caenorhabditis elegans.* Proc Natl Acad Sci U S A 72: 4061–4065.

Herman RK, Hedgecock EM (1990) Limitation of the size of the vulval primordium of *Caenorhabditis elegans* by *lin-15* expression in surrounding hypodermis. Nature 348:169–171.

Ignell R, Root CM, Birse RT, Wang JW, Nässel DR, Winther AM (2009) Presynaptic peptidergic modulation of olfactory receptor neurons in *Drosophila.* Proc Natl Acad Sci U S A 106:13070–13075.

Inada H, Ito H, Satterlee J, Sengupta P, Matsumoto K, Mori I (2006) Identification of guanylyl cyclases that function in thermosensory neurons of *Caenorhabditis elegans.* Genetics 172:2239–2252.

Jansen G, Thijssen KL, Werner P, van der Horst M, Hazendonk E, Plasterk RH (1999) The complete family of genes encoding G proteins of *Caenorhabditis elegans.* Nat Genet 21:414–419.

Jurado P, Kodama E, Tanizawa Y, Mori I (2010) Distinct thermal migration behaviors in response to different thermal gradients in *Caenorhabditis elegans.* Genes Brain Behav 9:120–127.

Kim K, Sato K, Shibuya M, Zeiger DM, Butcher RA, Ragains JR, Clardy J, Touhara K, Sengupta P (2009) Two chemoreceptors mediate developmental effects of dauer pheromone in *C. elegans.* Science 326:994–998.

Kim K, Kim R, Sengupta P (2010) The HMX/NKX homeodomain protein MLS-2 specifies the identity of the AWC sensory neuron type via regulation of the *ceh-36 Otx* gene in *C. elegans.* Development 137:963–974.

Kimura KD, Miyawaki A, Matsumoto K, Mori I (2004) The *C. elegans* thermosensory neuron AFD responds to warming. Curr Biol 14:1291–1295.

Klass MR (1977) Aging in the nematode *Caenorhabditis elegans*: major biological and environmental factors influencing life span. Mech Ageing Dev 6:413–429.

Komatsu H, Mori I, Rhee JS, Akaike N, Ohshima Y (1996) Mutations in a cyclic nucleotide-gated channel lead to abnormal thermosensation and chemosensation in *C. elegans.* Neuron 17:707–718.

Koo PK, Bian X, Sherlekar AL, Bunkers MR, Lints R (2011) The robustness of *Caenorhabditis elegans* male mating behavior depends on the distributed properties of ray sensory neurons and their output through core and male-specific targets. J Neurosci 31:7497–7510.

Kuhara A, Okumura M, Kimata T, Tanizawa Y, Takano R, Kimura KD, Inada H, Matsumoto K, Mori I (2008) Temperature sensing by an olfactory neuron in a circuit controlling behavior of *C. elegans.* Science 320:803–807.

Macosko EZ, Pokala N, Feinberg EH, Chalasani SH, Butcher RA, Clardy J, Bargmann CI (2009) A hub-and-spoke circuit drives pheromone attraction and social behavior in *C. elegans.* Nature 458:1171–1175.

Maricq AV, Peckol E, Driscoll M, Bargmann CI (1995) Mechanosensory signalling in *C. elegans* mediated by the GLR-1 glutamate receptor. Nature 378:78–81.

Mori I, Ohshima Y (1995) Neural regulation of thermotaxis in *Caenorhabditis elegans.* Nature 376:344–348.

Nakai J, Ohkura M, Imoto K (2001) A high signal-to-noise Ca(2+) probe composed of a single green fluorescent protein. Nat Biotechnol 19:137–141.

Nakazato K, Mochizuki A (2009) Steepness of thermal gradient is essential to obtain a unified view of thermotaxis in *C. elegans.* J Theor Biol 260:56–65.

Okochi Y, Kimura KD, Ohta A, Mori I (2005) Diverse regulation of sensory signaling by *C. elegans* nPKC-epsilon/eta TTX-4. EMBO J 24:2127–2137.

Ortiz CO, Etchberger JF, Posy SL, Frøkjaer-Jensen C, Lockery S, Honig B, Hobert O (2006) Searching for neuronal left/right asymmetry: genome-wide analysis of nematode receptor-type guanylyl cyclases. Genetics 173:131–149.

Peckol EL, Troemel ER, Bargmann CI (2001) Sensory experience and sensory activity regulate chemosensory receptor gene expression in *C. elegans.* Proc Natl Acad Sci U S A 98:11032–11038.

Pocock R, Hobert O (2010) Hypoxia activates a latent circuit for processing gustatory information in *C. elegans.* Nat Neurosci 13:610–614.

Prinz AA, Bucher D, Marder E (2004) Similar network activity from disparate circuit parameters. Nat Neurosci 7:1345–1352.

Ramot D, MacInnis BL, Goodman MB (2008a) Bidirectional temperature-sensing by a single thermosensory neuron in *C. elegans.* Nat Neurosci 11:908–915.

Ramot D, MacInnis BL, Lee HC, Goodman MB (2008b) Thermotaxis is a robust mechanism for thermoregulation in *Caenorhabditis elegans* nematodes. J Neurosci 28:12546–12557.

Renden R, Berwin B, Davis W, Ann K, Chin CT, Kreber R, Ganetzky B, Martin TF, Broadie K (2001) *Drosophila* CAPS is an essential gene that regulates dense-core vesicle release and synaptic vesicle fusion. Neuron 31:421–437.

Reppert SM, Weaver DR (2002) Coordination of circadian timing in mammals. Nature 418:935–941.

Ryu WS, Samuel AD (2002) Thermotaxis in *Caenorhabditis elegans* analyzed by measuring responses to defined thermal stimuli. J Neurosci 22:5727–5733.

Saideman SR, Blitz DM, Nusbaum MP (2007) Convergent motor patterns from divergent circuits. J Neurosci 27:6664–6674.

Sarafi-Reinach TR, Sengupta P (2000) The forkhead domain gene *unc-130* generates chemosensory neuron diversity in *C. elegans.* Genes Dev 14:2472–2485.

Satterlee JS, Sasakura H, Kuhara A, Berkeley M, Mori I, Sengupta P (2001) Specification of thermosensory neuron fate in *C. elegans* requires *ttx-1,* a homolog of *otd/Otx.* Neuron 31:943–956.

Satterlee JS, Ryu WS, Sengupta P (2004) The CMK-1 CaMKI and the TAX-4 cyclic nucleotide-gated channel regulate thermosensory neuron gene expression and function in *C. elegans.* Curr Biol 14:62–68.

Schackwitz WS, Inoue T, Thomas JH (1996) Chemosensory neurons function in parallel to mediate a pheromone response in *C. elegans.* Neuron 17:719–728.

Sieburth D, Ch'ng Q-L, Dybbs M, Tavazoie M, Kennedy S, Wang D, Dupuy D, Rual J-F, Hill DE, Vidal M, Ruvkun G, Kaplan JM (2005) Systematic analysis of genes required for synapse structure and function. Nature 436:510–517.

Sieburth D, Madison JM, Kaplan JM (2007) PKC-1 regulates secretion of neuropeptides. Nat Neurosci 10:49–57.

Speese S, Petrie M, Schuske K, Ailion M, Ann K, Iwasaki K, Jorgensen EM, Martin TF (2007) UNC-31 (CAPS) is required for dense-core vesicle but not synaptic vesicle exocytosis in *Caenorhabditis elegans.* J Neurosci 27:6150–6162.

Tang LS, Goeritz ML, Caplan JS, Taylor AL, Fisek M, Marder E (2010) Precise temperature compensation of phase in a rhythmic motor pattern. PLoS Biol 8:e1000469.

Tomioka M, Adachi T, Suzuki H, Kunitomo H, Schafer WR, Iino Y (2006) The insulin/PI 3-kinase pathway regulates salt chemotaxis learning in *Caenorhabditis elegans.* Neuron 51:613–625.

Tononi G, Sporns O, Edelman GM (1999) Measures of degeneracy and redundancy in biological networks. Proc Natl Acad Sci U S A 96:3257–3262.

Tsunozaki M, Chalasani SH, Bargmann CI (2008) A behavioral switch: cGMP and PKC signaling in olfactory neurons reverses odor preference in *C. elegans.* Neuron 59:959–971.

van der Linden AM, Beverly M, Kadener S, Rodriguez J, Wasserman S, Rosbash M, Sengupta P (2010) Genome-wide analysis of light- and temperature-entrained circadian transcripts in *Caenorhabditis elegans.* PLoS Biol 8:e1000503.

Wagner A (2005) Distributed robustness versus redundancy as causes of mutational robustness. Bioessays 27:176–188.

Wagner A, Wright J (2007) Alternative routes and mutational robustness in complex regulatory networks. Biosystems 88:163–172.

Wasserman SM, Beverly M, Bell HW, Sengupta P (2011) Regulation of response properties and operating range of the AFD thermosensory neurons by cGMP signaling. Curr Biol 21:353–362.

Whitacre JM (2010) Degeneracy: a link between evolvability, robustness and complexity in biological systems. Theor Biol Med Model 7:6.

Whitacre JM, Bender A (2010) Networked buffering: a basic mechanism for distributed robustness in complex adaptive systems. Theor Biol Med Model 7:20.

White JG, Southgate E, Thomson JN, Brenner S (1986) The structure of the nervous system of the nematode *Caenorhabditis elegans.* Philos Trans R Soc Lond B Biol Sci 314:1–340.

Wittenburg N, Baumeister R (1999) Thermal avoidance in *Caenorhabditis elegans*: an approach to the study of nociception. Proc Natl Acad Sci U S A 96:10477–10482.

Yamada Y, Ohshima Y (2003) Distribution and movement of *Caenorhabditis elegans* on a thermal gradient. J Exp Biol 206:2581–2593.

Yu S, Avery L, Baude E, Garbers DL (1997) Guanylyl cyclase expression in specific sensory neurons: A new family of chemosensory receptors. Proc Natl Acad Sci U S A 94:3384–3387.

Zariwala HA, Miller AC, Faumont S, Lockery SR (2003) Step response analysis of thermotaxis in *Caenorhabditis elegans.* J Neurosci 23:4369–4377.